

A structural and theoretical study of the intermolecular interactions in 8-hydroxyquinolinium-7-carboxylate monohydrate

Rafal Kruszynski

Institute of General and Ecological Chemistry, Technical University of Łódź,
ul. Żeromskiego 116, 90-924 Łódź, Poland
Correspondence e-mail: rafal.kruszynski@p.lodz.pl

Received 26 April 2011

Accepted 4 June 2011

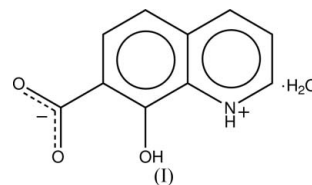
Online 17 June 2011

In the title compound, $C_{10}H_7NO_3 \cdot H_2O$, the zwitterionic organic molecules and the water molecules are connected by $N-H \cdots O$ and $O-H \cdots O$ hydrogen bonds to form ribbons, and $\pi-\pi$ stacking interactions expand these ribbons into a three-dimensional net. The energies of these hydrogen bonds adopt values typical for mildly weak interactions (3.33–7.75 kcal mol⁻¹; 1 kcal mol⁻¹ = 4.184 kJ mol⁻¹). The total $\pi-\pi$ stacking interactions between aromatic molecules can be classified as mildly strong (energies of 15.3 and 33.9 kcal mol⁻¹), and they are made up of multiple constituent $\pi-\pi$ interactions between six-membered rings. The short intermolecular $C-H \cdots O$ contact between two zwitterionic molecules is nonbonding in character.

Comment

The phenomenon of intermolecular interactions is essential in almost all chemical and biochemical processes (including catalysis and molecular assembly), and thus it is crucial in chemical and crystal engineering, as well as in supramolecular chemistry (Jeffrey & Saenger, 1991; Jeffrey, 1997; Epstein & Shubina, 2002). Since the beginning of the twentieth century, various types of intermolecular interactions (hydrogen and halogen bonds, $\pi-\pi$, anion– π and cation– π interactions, *etc.*) have been found and widely studied (Payer *et al.*, 2007; Schnabel *et al.*, 2007), including their spectroscopic (Tonge *et al.*, 2007; Fecko *et al.*, 2003), structural (Suresh, 2007; Fisher *et al.*, 2007) and thermodynamic (Harmon & Nikolla, 2003; Villar *et al.*, 2003) features. Careful inspection of the literature shows that the energetic behaviour of different intermolecular interactions has not been as commonly studied as other properties, although the number of reports on this topic has recently grown extensively. The energetic characteristics of such interactions are essential because they govern the stability of the assemblies formed (both supramolecular complexes and in-reaction intermediates), and as a conse-

quence they determine the possible applications of specific intermolecular interactions in chemical and biochemical processes (Gavezzotti, 2008; Oliveira *et al.*, 2006).



The title compound, (I), and its simple derivatives have diverse applications in pharmacy, medicine, agriculture and environmental protection. They possess potent antiviral activity against DNA herpes viruses, including cytomegalovirus, *Varicella zoster* virus, the Epstein–Barr virus, *Herpes simplex* virus and human herpes virus type 8 (Vaillancourt *et al.*, 1998). Additionally, they are effective in preventing RNA retroviruses (mainly human immunodeficiency viruses) from replicating (Haugwitz *et al.*, 1996) and they are efficient anti-tubercular agents (Urbanski, 1953). Because of its multi-dentate coordination ability, (I) and its chemical modifications are used as chelants for metals contaminating the environment. The simple and complex salts of (I) are also used as plant nutrients (Baret *et al.*, 1995). It must be noted that the mechanism of biological activity of (I) is still unresolved, and thus the study of its intermolecular bonding properties may be crucial for both determining the action mechanism and designing drugs of greater efficiency.

Reports of the structures of coordination compounds of (I) and its derivatives possessing a substituted N or O atom are extremely limited and only three compounds are known to date, namely dichloridooxido(8-oxidoquinoline-7-carboxylic acid)(triphenylphosphine)rhenium(V) triphenylphosphine oxide (Machura *et al.*, 2008), dibromidooxido(8-oxidoquinoline-7-carboxylic acid)(triphenylphosphine)rhenium(V) (Machura *et al.*, 2008) and hexakis(μ_2 -7-ethoxycarbonyl-8-oxyquinolinato)trilithiumdinickel(II) hydrogen sulfate diethyl ether solvate (Albrecht *et al.*, 2007).

The asymmetric unit of (I) contains one 8-hydroxyquinolinium-7-carboxylate zwitterion and one water molecule (Fig. 1). The zwitterionic form, which is typical for amino acids, has also been observed for only one structurally characterized isomer of (I), namely 8-hydroxyquinolinium-2-carboxylate, (II) (Okabe & Muranishi, 2002*b*). It must be mentioned that, in contrast with (I), (II) is solvent-free. For (II), structurally characterized coordination compounds are also almost unknown, and only seven such compounds have been studied to date, namely diaqua(8-oxidoquinoline-2-carboxylato-*N,O,O'*)copper(II) (Nakamura *et al.*, 2005), dichloridooxido(8-oxidoquinoline-2-carboxylic acid)(triphenylarsine)rhenium(V) acetonitrile solvate (Machura & Kusz, 2008), dichloridooxido(8-oxidoquinoline-2-carboxylic acid)(triphenylphosphine)rhenium(V) (Machura & Kusz, 2008), bis(8-hydroxyquinoline-2-carboxylato- $\kappa^3 O^2, N, O^8$)cobalt(II) trihydrate (Okabe & Muranishi, 2002*a*), bis(8-hydroxyquinoline-2-carboxylato- $\kappa^3 O^2, N, O^8$)nickel(II) trihydrate (Okabe & Muranishi, 2002*b*), bis(8-hydroxyquinoline-2-carboxylato- $\kappa^3 O^2, N,$

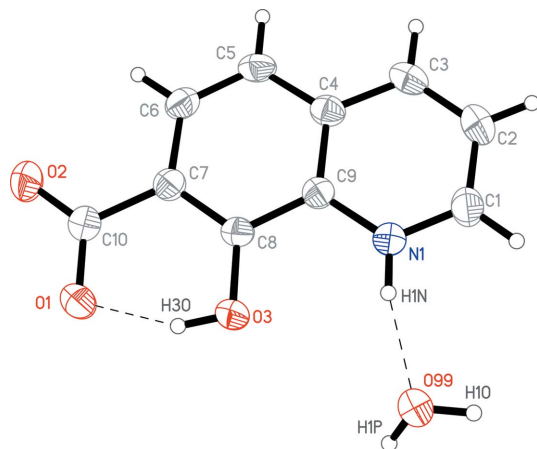


Figure 1

A view of the asymmetric unit of (I), showing the atom-labelling scheme. Displacement ellipsoids are drawn at the 50% probability level. Hydrogen bonds are indicated by dashed lines.

O^8)cadmium(II) trihydrate (McDonald *et al.*, 2008) and bis(8-hydroxyquinoline-2-carboxylato- $\kappa^3 O^2, N, O^8$)zinc(II) trihydrate (McDonald *et al.*, 2008). The above-mentioned zinc, cadmium, nickel and cobalt coordination compounds containing the 8-hydroxyquinoline-2-carboxylate moiety are isomorphous in the solid state.

The cyclic molecule of (I) is slightly distorted from planarity, with a maximum deviation from the weighted least-squares plane calculated for its all non-H atoms of 0.0281 (8) Å for atom O1. The corresponding maximum deviation in (II) also occurs for a carboxylate O atom, but it is distinctly larger (0.164 Å; Okabe & Muranishi, 2002*b*). The water molecule of (I) lies in the above-mentioned plane of the organic molecule [deviation = 0.0043 (14) Å]. The ten-membered ring systems have very similar bond lengths, which suggests almost perfect π -electron delocalization within them. These bond lengths in (I) differ by less than 0.03 Å from the analogous bond lengths of (II) and by less than 0.02 Å compared with values found for 8-hydroxyquinoline (Banerjee & Saha, 1986; Zhang & Wu, 2005). This proves that the delocalization is so strong that even protonation or deprotonation of the quinoline N atom does not affect the aromatic system. This postulation is confirmed by analysis of the UV spectra of (I) in neutral, acidic and basic environments. In each case, the band associated with the aromatic–aromatic $\pi \rightarrow \pi^*$ transition is unchanged, even in the N-deprotonated form of (I) (for details, see the *Experimental* section).

The molecules of (I) are held together by intermolecular N–H...O and O–H...O hydrogen bonds (Fig. 2 and Table 1) and π – π stacking interactions (Fig. 3 and Table 2). These hydrogen bonds, together with an intramolecular O–H...O interaction (Table 1), create a *DDDS*(6) unitary graph set (Bernstein *et al.*, 1995). At the secondary level graph, N_2 , the hydrogen bonds can be expressed as $R_4^+(12)D[R_4^+(18)D]-[C_2^2(9)D]$ basic graph sets. In this way, a ribbon parallel to the crystallographic [001] axis is created. Neighbouring layers are interlinked by π – π stacking interactions to form a three-dimensional net. There are also short intermolecular C–

H...O contacts (Table 1) present in the crystal structure, and on the basis of geometric considerations these can be classified as weak hydrogen bonds (Desiraju & Steiner 1999). However, the geometric parameters are misleading in this case, and this contact has a nonbonding nature. The hydrogen-bonding scheme in (II) is distinctly different (all motifs are infinite on the N_1 level), mainly due to the absence of any solvent molecule and, as a consequence, the absence of one hydrogen-bond acceptor and two hydrogen-bond donors. Some of the ring-centroid distances (Table 2) between stacked rings are longer than normal (Hunter & Sanders, 1990) but such elongation does not change their bonding character.

The hydrogen-bond energies in (I) lie in the ranges observed for similar non-ionic systems such as aminonitromethylbenzenes (Kruszynski & Sieranski, 2011), and they are lower than the energies of analogous hydrogen bonds formed in ionic species containing both organic and inorganic ions, *e.g.* 2,4-dinitrophenylhydrazine hydrochloride hydrate (Kruszynski, 2008), *o*-toluidinium dichloride dihydrate (Kruszynski, 2009), 2,3-dihydro-1,3-benzothiazol-2-iminium monohydrogen sulfate and 2-iminio-2,3-dihydro-1,3-benzothiazole-6-sulfonate (Kruszynski & Trzesowska-Kruszynska, 2009), 2-amino-5-chloro-1,3-benzoxazol-3-ium inorganic salts (Kruszynski & Trzesowska-Kruszynska, 2010), and 2,3-dihydro-1,3-benzothiazol-2-iminium hydrogen oxydiacetate (Trzesowska-Kruszynska & Kruszyński, 2009). This difference suggests that a significant increase in hydrogen-bond energies originates mainly from the overall molecular charge, not from local charges situated on particular atoms. It was previously found (for ionic species, *e.g.* nicotinothiazide dihydrochloride; Kruszyński, 2011) that stronger hydrogen bonds are created by anions acting as hydrogen-bond acceptors, and the strength of the interactions does not depend significantly on the charge located on the hydrogen-bond donors, *i.e.* neutral and cationic donors create bonds of similar strength (for the same acceptor and similar interaction geometry), while anionic acceptors create distinctly stronger interactions than neutral acceptors

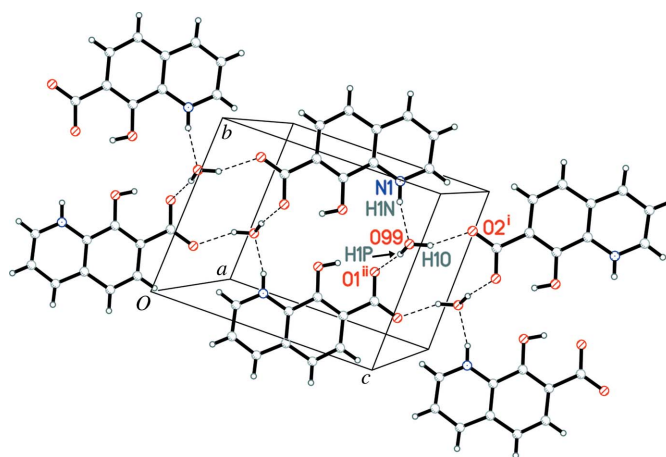


Figure 2

Part of the molecular packing of (I), showing the hydrogen-bonded ribbon parallel to the crystallographic [001] axis. Intermolecular hydrogen bonds are indicated by dashed lines. (Symmetry codes are as given in Table 1.)

interacting with the same donors and possessing similar hydrogen-bond geometry (Kruszynski, 2008, 2011). An analogous situation is observed for the neutral molecule of (I), possessing local charges (Breneman & Wiberg, 1990) situated on the N1–H1N group [0.97 (1) a.u.] and on atoms O1 and O2 [−0.75 (4) a.u.]. In general, all bonds can be classified as mildly weak, but the shorter N⁺–H···O intermolecular hydrogen bonds are less than half the strength of the longer O–H···O[−] hydrogen bonds (Table 1). Thus, it can again be stated that for the creation of stronger hydrogen bonds, the additional electron density on a hydrogen-bond acceptor is more important than the electron-density deficiency on a hydrogen-bond donor, although for neutral molecules these energy differences are not large. It must be noted that the geometrically allowed (Desiraju & Steiner, 1999) C1–H1···O2ⁱ hydrogen bond (symmetry code given in Table 1) is actually a nonbonding interaction. The total strength of the intramolecular O3–H3O···O1 interaction (estimated as described in the *Experimental* section) is 2.47 kcal mol^{−1} (1 kcal mol^{−1} = 4.184 kJ mol^{−1}). Calculation of the intermolecular interaction energies of parallel aromatic 12-membered ring systems related by the symmetry transformations (−*x* + 1, −*y* + 2, −*z* + 1) and (−*x*, −*y* + 2, −*z* + 1) shows that these interactions are bonding in character with energies of 15.3 (7) and 33.9 (9) kcal mol^{−1}, respectively. The differences between calculations excluding and including the dispersion energy, E_{disp} , are no more than 1.1 kcal mol^{−1} ($E_{\text{DFT}} < E_{\text{MP2}}$), which proves that this energy is involved in these interactions although its contribution is small ($E_{\text{disp}} < 5\% E$). The total intermolecular interaction (with the above-mentioned energy) is made up of multiple π – π stacking interactions between neighbouring six-membered rings (four pairs of six-membered rings in the first case and three pairs in the second; Table 2).

The noncovalent nature of the intermolecular interactions in (I) was analysed using the natural bond orbital (NBO) method (Foster & Weinhold, 1980; Reed & Weinhold, 1985; Reed *et al.*, 1988). In this method, the strength of the donor–acceptor charge-transfer delocalization is characterized by the second-order stabilization energy, E_{del} . For hydrogen bonds, the principal charge-transfer interactions $E_{\text{del}}(1)$ (Table 1) occur between the lone electron pairs of the O atoms and the antibonding orbitals of the N–H and O–H bonds. In the lateral charge-transfer interactions, the lone electron pairs of the O atoms donate their electron density to the one-centre Rydberg orbitals of the H atoms. The stacking interactions are formed by the bonding π orbitals of one ring donating electron density primarily to the antibonding π orbitals of the second ring [$E_{\text{del}}(1)$ in Table 2] and secondarily to the one-centre Rydberg antibonding orbitals of the π -bonded atoms of the rings. The first-mentioned orbitals interactions contribute about 70–80% of the total energy of the π – π interactions. This dependence is also observed for the intermolecular interaction energy of parallel aromatic ring systems related by the symmetry transformations (−*x* + 1, −*y* + 2, −*z* + 1) and (−*x*, −*y* + 2, −*z* + 1), in which the primary NBO interactions characterized by $E_{\text{del}}(1)$ are responsible for 68% (10.4 out of a

total of 15.3 kcal mol^{−1}) and 82% (27.8 out of 33.9 kcal mol^{−1}) of the total intermolecular interactions, respectively. The observed energies of the stacking interactions between six-membered rings lie in the ranges for both real and idealized systems [e.g. similar π – π stacking interactions were estimated to be 0.59 kcal mol^{−1} for 2,3-dimethyl-6-nitroaniline (Kruszynski & Sieranski, 2011), 1.32 kcal mol^{−1} for the solid-state benzene dimer (Rubes & Bludsky, 2008) and 8.7 kcal mol^{−1} for the histidine-substituted uracil dimer (Cysewski, 2008)]. It is noteworthy that a geometric arrangement of the benzene and pyridine moieties in which the distances between the ring centroids are close to 5 Å still leads to bonding π – π interactions (Table 2). The systematic study of aminonitromethylbenzenes shows that such a long distance typically leads to a nonbonding interaction (Kruszynski & Sieranski, 2011). Thus, it can be postulated that a synergistic effect with other π – π interactions between fused rings is required to form such a long bonding interaction.

Experimental

Compound (I) was synthesized according to the modified procedure of Meek & Fuchsmann (1969). Equimolar amounts (0.1 mol) of 8-hydroxyquinoline and NaOH (analytical grade, POCh Gliwice) were placed in a two-necked round-bottomed flask and toluene (50 ml) was added. The flask was mounted in a Dean–Stark apparatus for solvents with a density less than water and the solution was heated at boiling for 3 h. Next, the solution was cooled to 353 K, the flask was removed from the Dean–Stark apparatus and *N,N*-dimethylformamide (50 ml) was added to the solution. A bubbler was mounted in the side neck of the flask and a still head with a condenser was fitted to the main neck. The solution was heated to 418 K (the toluene starts to distil at about 383 K) and at this temperature CO₂ was passed through the solution *via* the bubbler. Next, the solution was heated to 433 K and kept at this temperature for 3 h with CO₂ continuously flowing through it. After this period of time, the solution was cooled and poured into water (150 ml). The solid residue was filtered off and the solution was acidified to pH 4.0 with concentrated HCl. The precipitate which formed, containing (I) and small amounts of 7-carboxy-8-hydroxyquinoline hydrochloride, was filtered off and dissolved in a 0.01 M solution of NaOH in water–methanol (1:1 *v/v*; 100 ml). Good quality yellow crystals of (I) grew from this solution after 6 h.

UV–Vis data [wavelength (nm), molar extinction coefficient (m² mol^{−1}), transition character; – indicates the parameter is not applicable] for (I). In aqueous solution: 210 (s), 4212.7, $\pi(\text{COO}) \rightarrow \pi^*(\text{COO})$; 218 (w), 1767.2, $\pi(\text{COO}) \rightarrow \pi^*(\text{COO})$; 257 (s), 4747.9, $p(\text{aromatic}) \rightarrow \pi^*(\text{aromatic})$; 315 (w), 300.9, $n \rightarrow \pi^*(\text{COO})$; 333 (w), 265.1, $n \rightarrow \pi^*(\text{aromatic})$. In the solid state: 232 (s), –, $p(\text{aromatic}) \rightarrow \pi^*(\text{aromatic})$; 278 (w), –, $n \rightarrow \pi^*(\text{COO})$; 331 (w), –, $n \rightarrow \pi^*(\text{aromatic})$; 360 (s), –, intramolecular $p(\text{aromatic}) \rightarrow \pi^*(\text{aromatic})$; 404 (w), –, intramolecular $p(\text{aromatic}) \rightarrow \text{Ry}^*(\text{aromatic})$. In 6 M hydrochloric acid–water solution: 205 (s), 20549.4, $\pi(\text{COO}) \rightarrow \pi^*(\text{COO})$; 217 (w), 1198.0, $\pi(\text{COO}) \rightarrow \pi^*(\text{COO})$; 265 (s), 4520.3, $p(\text{aromatic}) \rightarrow \pi^*(\text{aromatic})$; 309 (s), 193.4, $n \rightarrow \pi^*(\text{COO})$; 356 (s), 216.6, $n \rightarrow \pi^*(\text{aromatic})$. In 10 M ammonium hydroxide–water solution: 197 (w), 869.4, $\pi(\text{COO}) \rightarrow \pi^*(\text{COO})$; 206 (w), 1141.9, $\pi(\text{COO}) \rightarrow \pi^*(\text{COO})$; 216 (w), 1269.0, $\pi(\text{COO}) \rightarrow \pi^*(\text{COO})$; 255 (s), 3493.7, $p(\text{aromatic}) \rightarrow \pi^*(\text{aromatic})$; 311 (s), 261.4, $n \rightarrow \pi^*(\text{COO})$; 329 (s), 302.1, $n \rightarrow \pi^*(\text{aromatic})$.

Table 1

Experimental hydrogen-bond geometry for (I) (Å, °), total energy E (kcal mol⁻¹) and principal 'delocalization' energy $E_{\text{del}}(1)$, calculated on the NBO basis.

See *Comment* for a detailed description of the abbreviations and methods used.

$D-H\cdots A$	$D-H$	$H\cdots A$	$D\cdots A$	$D-H\cdots A$	E	$E_{\text{del}}(1)$
N1—H1N ⁱ ···O99	0.86	1.82	2.6548 (13)	165.8	3.33	2.74
O3—H3O ⁱ ···O1	0.87	1.65	2.4692 (11)	154.7		1.64
O99—H1O ⁱ ···O2 ⁱ	0.87	1.88	2.7027 (13)	157.8	7.03	6.40
O99—H1P ⁱ ···O1 ⁱⁱ	0.84	1.92	2.7513 (13)	171.1	7.45	6.18
C1—H1 ⁱ ···O2 ⁱ	0.93	2.34	3.1934 (16)	152.8	Non-bonding interaction	

Symmetry codes: (i) $x, y, z + 1$; (ii) $-x + 1, -y + 1, -z + 1$.

Crystal data

$C_{10}H_7NO_3 \cdot H_2O$	$\gamma = 73.083 (5)^\circ$
$M_r = 207.18$	$V = 457.76 (5) \text{ \AA}^3$
Triclinic, $P\bar{1}$	$Z = 2$
$a = 7.0045 (4) \text{ \AA}$	Mo $K\alpha$ radiation
$b = 7.6512 (5) \text{ \AA}$	$\mu = 0.12 \text{ mm}^{-1}$
$c = 9.4192 (5) \text{ \AA}$	$T = 291 \text{ K}$
$\alpha = 87.877 (5)^\circ$	$0.02 \times 0.01 \times 0.01 \text{ mm}$
$\beta = 71.718 (5)^\circ$	

Data collection

Kuma KM-4 CCD area-detector diffractometer	4445 measured reflections
Absorption correction: numerical (<i>X-RED</i> ; Stoe & Cie, 1999)	1608 independent reflections
$T_{\text{min}} = 0.997, T_{\text{max}} = 1.000$	1230 reflections with $I > 2\sigma(I)$
	$R_{\text{int}} = 0.031$

Refinement

$R[F^2 > 2\sigma(F^2)] = 0.032$	136 parameters
$wR(F^2) = 0.092$	H-atom parameters constrained
$S = 0.99$	$\Delta\rho_{\text{max}} = 0.15 \text{ e \AA}^{-3}$
1608 reflections	$\Delta\rho_{\text{min}} = -0.25 \text{ e \AA}^{-3}$

The molecular electronic properties (Tables 1 and 2) were calculated at a single point for both the diffraction-derived coordinates and the optimized structure, and these are comparable within four standard deviations, although the geometrically optimized molecules show a typical elongation of the O—H, N—H and C—H bonds (from 0.06 to 0.19 Å). The total binding energies of the intermolecular interactions were calculated for molecular sets containing from one to 16 molecules using the total self-consistent field energy. The molecules within each molecular set were arranged in hydrogen-bonded ribbons (an example of such a ribbon for the ten-molecule set is depicted in Fig. 2) and in piles formed by π – π interactions. The structural parameters (with H-atom positions geometrically optimized) were the starting model in each calculation. Basis set superposition error (BSSE) corrections were carried out using the counterpoise (CP) method (Boys & Bernardi, 1970). The B3LYP functional (Becke, 1993; Lee *et al.*, 1988) and Hartree–Fock calculation, followed by a Møller–Plesset correlation energy correction (Møller & Plesset, 1934) truncated at the second order (Head-Gordon *et al.*, 1988) in the triple- ζ 6-311++G(3df,2p) basis set was used, as implemented in *GAUSSIAN03* (Frisch *et al.*, 2004). In all cases, the differences in electronic properties and energies originating from the different number of molecules used in the calculation, and the differences between the above-described methods, are given in parentheses as standard deviations of the mean values. Where a

Table 2

Experimental stacking interaction geometry (Å, °) for (I) and principal 'delocalization' energies (kcal mol⁻¹) for $CgJ \rightarrow CgK$ [$E_{\text{del}}(1, J \rightarrow K)$] and $CgK \rightarrow CgJ$ [$E_{\text{del}}(1, K \rightarrow J)$] transitions, calculated on the MP2-NBO basis.

CgN and CgC are the ring centroids of the six-membered pyridine and benzene rings, respectively. $Cg\cdots Cg$ is the distance between the first ring centroid and that of the second ring, α is the dihedral angle between planes J and K , β is the angle between the vector linking the ring centroid and the normal to ring J , and CgJ_{perp} is the perpendicular distance from the J ring centroid to ring K .

$CgJ\cdots CgK$	$Cg\cdots Cg$	α	β	CgJ_{perp}	$E_{\text{del}}(1, J \rightarrow K)$	$E_{\text{del}}(1, K \rightarrow J)$
$CgN\cdots CgN^{\text{iii}}$	4.9826 (16)	0	47.61 (12)	3.3594 (15)	0.96	0.96
$CgN\cdots CgC^{\text{iii}}$	3.6427 (18)	0.615 (11)	23.35 (11)	3.3287 (18)	1.61	1.48
$CgC\cdots CgN^{\text{iii}}$	3.6427 (18)	0.615 (11)	23.96 (11)	3.3444 (18)	1.48	1.61
$CgC\cdots CgC^{\text{iii}}$	3.6413 (19)	0	23.67 (11)	3.3350 (18)	1.16	1.16
$CgN\cdots CgC^{\text{iv}}$	4.7996 (18)	0.615 (11)	45.87 (11)	3.3774 (18)	3.23	3.10
$CgC\cdots CgN^{\text{iv}}$	4.7996 (18)	0.615 (11)	45.28 (11)	3.3418 (18)	3.10	3.23
$CgC\cdots CgC^{\text{iv}}$	3.6505 (19)	0	22.56 (11)	3.3711 (18)	7.58	7.58

Symmetry codes: (iii) $-x + 1, -y + 2, -z + 1$; (iv) $-x, -y + 2, -z + 1$.

deviation is not given, the values were the same within their range of reported precision. The total strength of the intramolecular O3—H3Oⁱ···O1 hydrogen bond cannot be calculated by total self-consistent field energy due to the impossibility of dividing the molecule into two closed-shell systems. Thus, it was estimated by summation over all elements of the second-order perturbation theory analysis of the Fock matrix [on the NBO basis (Foster & Weinhold, 1980; Reed & Weinhold, 1985; Reed *et al.*, 1988)] associated with this interaction.

C-bound H atoms were placed in calculated positions (C—H = 0.93 Å) and other H atoms were found from the difference Fourier syntheses after eight cycles of anisotropic refinement (N—H and O—H distances are as in Table 1). All H atoms were refined as riding on their parent atoms, with $U_{\text{iso}}(\text{H}) = 1.2U_{\text{eq}}(\text{C}, \text{N})$ or $1.5U_{\text{eq}}(\text{O})$, in all refinement cycles (including the final one). The isotropic displacement parameters of O- and N-bound H atoms were then refined to check the correctness of their positions in the post-final calculation. After eight cycles, the refinement reached stable convergence with isotropic displacement parameters in the range 0.053–0.084 Å⁻². The values of the isotropic displacement parameters of the H atoms have reasonable values (compared with their parent non-H atoms), which proves the correctness of the H-atom positions.

Data collection: *CrysAlis CCD* (Oxford Diffraction, 2006); cell refinement: *CrysAlis RED* (Oxford Diffraction, 2006); data reduction: *CrysAlis RED*; program(s) used to solve structure: *SHELXS97* (Sheldrick, 2008); program(s) used to refine structure: *SHELXL97* (Sheldrick, 2008); molecular graphics: *XP* in *SHELXTL/PC* (Sheldrick, 2008) and *ORTEP-3 for Windows* (Version 1.062; Farrugia, 1997); software used to prepare material for publication: *SHELXL97* and *PLATON* (Spek, 2008).

The author expresses his sincere thanks to Professor Barbara Machura for providing a reagent. This work was financed by funds allocated by the Ministry of Science and Higher Education to the Institute of General and Ecological Chemistry, Technical University of Lodz. The *GAUSSIAN03* calculations were carried out in the Academic Computer Centre ACK CYFRONET of the University of Science and Technology (AGH) in Cracow, Poland, under grant No. MNiSW/SGI3700/PŁódzka/040/2008.

Supplementary data for this paper are available from the IUCr electronic archives (Reference: UK3030). Services for accessing these data are described at the back of the journal.

References

- Albrecht, M., Fiege, M., Baumert, M., de Groot, M., Frohlich, R., Russo, L. & Rissanen, K. (2007). *Eur. J. Inorg. Chem.* pp. 609–616.
- Banerjee, T. & Saha, N. N. (1986). *Acta Cryst.* **C42**, 1408–1411.
- Baret, P., Caris, C., Laulhere, J.-P. & Pierre, J.-L. (1995). World Patent WO/1995/012580.
- Becke, A. D. (1993). *J. Chem. Phys.* **98**, 5648–5652.
- Bernstein, J., Davis, R. E., Shimoni, L. & Chang, N.-L. (1995). *Angew. Chem. Int. Ed. Engl.* **34**, 1555–1573.
- Boys, S. F. & Bernardi, F. (1970). *Mol. Phys.* **19**, 553–566.
- Breneman, C. M. & Wiberg, K. B. (1990). *J. Comput. Chem.* **11**, 361–373.
- Cysewski, P. (2008). *Phys. Chem. Chem. Phys.* **10**, 2636–2645.
- Desiraju, G. R. & Steiner, T. (1999). *The Weak Hydrogen Bond in Structural Chemistry and Biology*. New York: Oxford University Press Inc.
- Epstein, L. M. & Shubina, E. S. (2002). *Coord. Chem. Rev.* **231**, 165–181.
- Farrugia, L. J. (1997). *J. Appl. Cryst.* **30**, 565.
- Fecko, C. J., Eaves, J. D., Loparo, J. J., Tokmakoff, A. & Geissler, P. L. (2003). *Science*, **301**, 1698–1702.
- Fisher, S. Z., Anderson, S., Henning, R., Moffat, K., Langan, P., Thiyagarajan, P. & Schultz, A. J. (2007). *Acta Cryst.* **D63**, 1178–1184.
- Foster, J. P. & Weinhold, F. A. (1980). *J. Am. Chem. Soc.* **102**, 7211–7218.
- Frisch, M. J., *et al.* (2004). *GAUSSIAN03*. Revision E.01. Gaussian Inc., Wallingford, Connecticut, USA.
- Gavezzotti, A. (2008). *Acta Cryst.* **B64**, 401–403.
- Harmon, K. H. & Nikolla, E. (2003). *J. Mol. Struct.* **657**, 117–123.
- Haugwitz, R. D., Zalkow, L., Gruszecka-Kowalik, E. & Burgess, E. (1996). World Patent WO/1996/025399.
- Head-Gordon, M., Pople, J. A. & Frisch, M. J. (1988). *Chem. Phys. Lett.* **153**, 503–506.
- Hunter, C. A. & Sanders, J. K. M. (1990). *J. Am. Chem. Soc.* **112**, 5525–5534.
- Jeffrey, G. A. (1997). In *An Introduction to Hydrogen Bonding*. Oxford University Press.
- Jeffrey, G. A. & Saenger, W. (1991). In *Hydrogen Bonding in Biological Structures*. Heidelberg: Springer-Verlag.
- Kruszynski, R. (2008). *Cent. Eur. J. Chem.* **6**, 542–548.
- Kruszynski, R. (2009). *Pol. J. Chem.* **83**, 615–623.
- Kruszynski, R. (2011). *Acta Cryst.* **C67**, o52–o56.
- Kruszynski, R. & Sieranski, T. (2011). *Cent. Eur. J. Chem.* **9**, 94–105.
- Kruszynski, R. & Trzesowska-Kruszynska, A. (2009). *Acta Cryst.* **C65**, o624–o629.
- Kruszynski, R. & Trzesowska-Kruszynska, A. (2010). *Acta Cryst.* **C66**, o449–o454.
- Lee, C., Yang, W. & Parr, R. G. (1988). *Phys. Rev. B*, **37**, 785–789.
- Machura, B. & Kusz, J. (2008). *Polyhedron*, **27**, 366–374.
- Machura, B., Milek, J., Kusz, J., Nycz, J. & Tabak, D. (2008). *Polyhedron*, **27**, 1121–1130.
- McDonald, F. C., Applefield, R. C., Halkides, C. J., Reibenspies, J. H. & Hancock, R. D. (2008). *Inorg. Chim. Acta*, **361**, 1937–1946.
- Meek, W. H. & Fuchsman, C. H. (1969). *J. Chem. Eng. Data*, **14**, 388–391.
- Møller, C. & Plesset, M. S. (1934). *Phys. Rev.* **46**, 618–622.
- Nakamura, M., Kitamura, C., Ueyama, H., Yamana, K. & Yoneda, A. (2005). *Anal. Sci. X-Ray Struct. Anal. Online*, **21**, x115–x116.
- Okabe, N. & Muranishi, Y. (2002a). *Acta Cryst.* **E58**, m352–m353.
- Okabe, N. & Muranishi, Y. (2002b). *Acta Cryst.* **C58**, m475–m477.
- Oliveira, B. G., Pereira, F. S., de Araujo, R. C. M. U. & Ramos, M. N. (2006). *Chem. Phys. Lett.* **427**, 181–184.
- Oxford Diffraction (2006). *CrysAlis CCD and CrysAlis RED*. Versions 1.163. Oxford Diffraction Ltd, Abingdon, Oxfordshire, England.
- Payer, D., Comisso, A., Dmitriev, A., Strunskus, T., Lin, N., Woll, C., DeVita, A., Barth, J. V. & Kern, K. (2007). *Chem. Eur. J.* **13**, 3900–3906.
- Reed, A. E., Curtis, L. A. & Weinhold, F. A. (1988). *Chem. Rev.* **88**, 899–926.
- Reed, A. E. & Weinhold, F. A. (1985). *J. Chem. Phys.* **83**, 1736–1740.
- Rubes, M. & Bludsky, O. (2008). *Phys. Chem. Chem. Phys.* **10**, 2611–2615.
- Schnabel, T., Srivastava, A., Vrabc, J. & Hasse, H. J. (2007). *J. Phys. Chem. B*, **111**, 9871–9878.
- Sheldrick, G. M. (2008). *Acta Cryst.* **A64**, 112–122.
- Spek, A. L. (2009). *Acta Cryst.* **D65**, 148–155.
- Stoe & Cie (1999). *X-RED*. Version 1.18. Stoe & Cie GmbH, Darmstadt, Germany.
- Suresh, S. J. (2007). *J. Chem. Phys.* **126**, 204705.
- Tonge, N. M., MacMahon, E. C., Pugliesi, I. & Cockett, M. C. (2007). *J. Chem. Phys.* **126**, 154319.
- Trzesowska-Kruszynska, A. & Kruszynski, R. (2009). *Acta Cryst.* **C65**, o19–o23.
- Urbanski, T. (1953). *Bull. Acad. Pol. Sci. Cl. 3*, **1**, 319–323.
- Vaillancourt, V. A., Romines, K. R., Romero, A. G., Tucker, J. A., Strohbach, J. W., Bezencon, O. & Thaisrivongs, S. (1998). World Patent WO/1998/011073.
- Villar, V., Irusta, L., Fernandez-Berridi, M. J., Iruin, J. J., Iriarte, M., Gargallo, L. & Radic, D. (2003). *Thermochim. Acta*, **402**, 209–218.
- Zhang, J. & Wu, L. (2005). Private communication (refcode HXQUIN11). CCDC, Union Road, Cambridge, England.